

Research on the approximate equation inversion method for the physical properties parameters of OA media with decoupling of stress and fracture effects

Zihang Fan^{1, a}, Zhaoyun Zong^{1, b *}

¹ School of Earth Sciences and Technology, China University of Petroleum (East China), Qingdao Shandong, China;

^a zihang_fan@163.com, ^b zongzhaoyun@upc.edu.cn

Abstract. Pre-stack seismic inversion is an effective method for predicting reservoir physical parameters. At the same time, azimuth seismic data is a reliable source of information for predicting underground reservoir elastic parameters, fracture parameters, and interface parameters and has rich underground information. However, it is difficult to determine whether the anisotropy of the reservoir is caused by stress or the original fractures. Therefore, distinguishing the influence of fractures and initial stress in the reservoir from azimuth seismic data is the key to predicting reservoir parameters. Because of the problem of insufficient consideration of the influence of stress and fracture weakness in OA media, based on Born's first-order scattering theory and Bayesian inversion framework, an approximate equation for the reflection coefficient decoupling fracture anisotropy and stress-induced anisotropy was constructed, and a linear inversion method based on the approximate equation was developed, realizing the exploration of methods for predicting fracture weakness and stress action parameters. Model testing and actual work area application have verified the feasibility and practicability of predicting underground medium parameters from seismic response characteristics.

Keywords: OA media; Born approximation; Initial stress; Azimuth Amplitude Difference Method.

1. Introduction

Since underground reservoirs and media are generally subject to initial stress, and this effect will have a significant impact on the propagation of seismic waves, the acoustic, elastic theory is usually used to describe it in research [1-3]. In earlier studies based on static nonlinear wave theory and continuous medium theory, the study of large initial strains superimposed on minor disturbances made the acoustoelastic theory more perfect [4, 5]. Subsequently, the acoustoelastic theory has been widely used in the engineering field, mainly for measuring the residual stress of metals, monitoring the changes in the longitudinal and transverse wave velocities of metals induced by stress, calculating the third-order elastic modulus, and non-destructive testing of metal samples [6-7]. Breakthroughs were made in measuring the third-order elastic modulus of various dry sandstone samples. More importantly, the third-order elastic tensor of various rocks was measured [8], which confirmed that rocks have pronounced nonlinear characteristics and have better resolution and sensitivity than metals. This has extensively promoted the application of acoustoelastic theory in geophysical exploration and has attracted widespread attention from researchers in the field of exploration and development [9-11].

Seismic inversion is an effective way to obtain complex underground media's elastic and physical parameters. With the continuous development of oil and gas exploration technology, underground media are becoming increasingly complex, and the requirements for inversion are increasing. Therefore, the pre-stack seismic inversion method using azimuthal seismic data has become the mainstream application. On this basis, using the fracture reservoir prediction method, a direct prediction method for fracture density and fracture trend [12] was successfully proposed. Subsequently, the application scenarios of pre-stack seismic inversion methods have been extended to complex media for the inversion of fractures and ground stresses, such as heterogeneous media and unconventional gas-bearing reservoirs [13], based on different inversion parameters and

geological backgrounds. While the equations are being innovated, improving inversion algorithms also develop synchronously with theory. For example, the two-step AVA (Amplitude Variation with Azimuth) inversion method based on the two-step method uses the inversion results of small-angle data to predict anisotropic reservoirs [14], and a parameter prediction method for shale gas reservoirs using the combined longitudinal and transverse wave pre-stack method [15]. In addition to using the elastic parameters in the reflection coefficient equation to build a bridge between physical parameters and reflection coefficient, rock physics and seismic response are combined to propose an AVA inversion method for the physical parameters of fractured reservoirs [16].

Scholars at domestic and abroad have proposed various seismic inversion methods based on approximate equations for different media. However, there is still a problem because it is difficult to distinguish the anisotropy caused by initial stress and fractures. It is urgent to explore the reservoir parameter inversion method based on the approximate equation that considers the decoupling of stress and fracture effects that takes into account the initial stress, improve the actual fit of the approximate equation inversion model, verify the rationality of inverting complex medium reservoir parameters from the approximate reflection coefficient, and improve the efficiency of pre-stack seismic inversion of reservoir parameters.

2. Inversion of AVA approximate equation for PP waves in OA media based on initial stress

How to decouple stress and fracture effects, explore the physical property information within the layer, and realize the inversion of fracture and stress effects is an urgent problem to be solved. Based on the Bayesian inversion framework, the inversion method of azimuthal amplitude difference is adopted, and based on the first-order scattered elastic wave steady phase method, an approximate equation for decoupling stress and fracture parameters is developed, and a quantitative relationship between stress, fracture parameters and reflection coefficient in the medium is established, which improves the rationality of reservoir parameter prediction and is conducive to the feasibility analysis of shale reservoir exploration and development.

2.1 Construction of equivalent stiffness coefficient matrix for decoupling fracture and stress effects

Based on the weak anisotropy approximation, it is assumed that the changes caused by intrinsic anisotropy and stress are small perturbations imposed on a stress-free reference background. Assuming that there is only uniaxial stress on the y-axis, the anisotropic parameter of the stressed OA medium can be written as the sum of the unstressed OA medium and the stress term [17]:

$$\begin{aligned} \varepsilon_{OA_str}^{(1)} &= \varepsilon_b^{(1)} + \frac{K_p}{2c_{55}} \tau_{22}; & \gamma_{OA_str}^{(1)} &= \gamma_b^{(1)} + \frac{K_s}{2c_{55}} \tau_{22}; & \delta_{OA_str}^{(1)} &= \delta_b^{(1)} + \frac{K_p}{2c_{55}} \tau_{22}; \\ \gamma_{OA_str}^{(2)} &= \gamma_b^{(2)}; & \varepsilon_{OA_str}^{(2)} &= \varepsilon_b^{(2)}; & \delta_{OA_str}^{(2)} &= \delta_b^{(2)}; & \delta_{OA_str}^{(3)} &= \delta_b^{(3)} \end{aligned} \quad (1)$$

Where $\varepsilon_{OA_str}^{(1)}$, $\varepsilon_{OA_str}^{(2)}$, $\gamma_{OA_str}^{(1)}$, $\gamma_{OA_str}^{(2)}$, $\delta_{OA_str}^{(1)}$, $\delta_{OA_str}^{(2)}$, $\delta_{OA_str}^{(3)}$, represent the seven Thomson anisotropy parameters of the OA medium after considering the initial stress, the subscript b represents the anisotropy parameter without stress. K_p and K_s represent the longitudinal and transverse wave anisotropy parameters that control stress induction, respectively, which can be expressed as:

$$\begin{aligned}
K_p &= (C_{111} - C_{112}) / (c_{33}); \\
K_p &= (C_{111} - 3C_{112} + 2C_{123}) / (8c_{55}); \\
\Gamma_P &= \frac{K_p}{2c_{55}} \tau_{22}, \Gamma_S = \frac{K_s}{2c_{55}} \tau_{22}
\end{aligned} \tag{2}$$

c_{55} represents the elastic parameters of the OA medium under unstressed conditions, $\tau_{11}, \tau_{22}, \tau_{33}$ represents the initial stress, Γ_P and Γ_S represent the stress terms of P-wave and S-wave, respectively.

After obtaining the relationship between the stress action term and the anisotropic parameter, in order to simultaneously consider the effect of the fracture, the stress action term and the fracture parameter are combined using the relationship between the anisotropic parameter and the fracture parameter:

$$\begin{aligned}
\varepsilon_{OA}^{(1)} &= \varepsilon_{VTI}; & \varepsilon_{OA}^{(2)} &= \varepsilon_{VTI} - 2g(1-g)\Delta_N; \\
\delta_{OA}^{(1)} &= \delta_{VTI}; & \delta_{OA}^{(2)} &= \delta_{VTI} - 2g((1-2g)\Delta_N + \Delta_T); & \delta_{OA}^{(3)} &= 2g(\Delta_N - \Delta_H); \\
\gamma_{OA}^{(1)} &= \gamma_{VTI} + \frac{\Delta_T - \Delta_H}{2}; & \gamma_{OA}^{(2)} &= \gamma_{VTI} - \frac{\Delta_H}{2}
\end{aligned} \tag{3}$$

The anisotropic parameters are all parameters when there is no stress. The subscript VTI in the lower right corner of the equation represents the VTI medium without stress. Δ_N , Δ_T , and Δ_H represent the normal, tangential and transverse fracture weaknesses of the fracture, respectively.

According to equation (3), the conversion relationship between the fracture parameters and the anisotropic parameters can be obtained, and the three fracture weaknesses of the OA medium under the initial stress can be obtained. Then, combined with (1), the expressions of the fracture weakness without stress and the P-wave and S-wave stress terms are obtained:

$$\begin{cases} \Delta_N^{str} = \Delta_N + \frac{1}{2g(1-g)} \Gamma_P; \\ \Delta_T^{str} = \Delta_T + 2\Gamma_S; \\ \Delta_H^{str} = \Delta_H + \frac{1}{2g(1-g)} \Gamma_P \end{cases} \tag{4}$$

Since the equivalent elastic parameter under stress can be written as $C_{ijkl} = c_{ijkl} + c_{ijklmn}E_{mn}$, based on the equivalent stiffness matrix of OA medium under stress represented by background medium and fracture weakness, combined with (4), the equivalent stiffness matrix of OA medium under stress represented by fracture weakness and stress terms can be obtained:

$$\begin{aligned}
C_{11}^{OA-str} &\approx c_{11}(1-\Delta_N) + c_{11} \frac{1}{4g(1-g)} \Gamma_P; & C_{12}^{OA-str} &\approx c_{12}(1-\Delta_N) + c_{12} \frac{1}{4g(1-g)} \Gamma_P = C_{21}^{OA-str}; \\
C_{13}^{OA-str} &\approx c_{13}(1-\Delta_N) + c_{13} \frac{1}{4g(1-g)} \Gamma_P = C_{31}^{OA-str}; & C_{22}^{OA-str} &\approx c_{11} - \Delta_N \frac{c_{12}^2}{c_{11}} + \frac{c_{12}^2}{c_{11}} \frac{1}{4g(1-g)} \Gamma_P; \\
C_{23}^{OA-str} &\approx c_{13} \left(1 - \Delta_N \frac{c_{12}}{c_{11}} \right) + c_{13} \frac{1}{4g(1-g)} \Gamma_P \frac{c_{12}}{c_{11}} = C_{32}^{OA-str}; & C_{33}^{OA-str} &\approx c_{33} - \Delta_N \frac{c_{13}^2}{c_{11}} + \frac{c_{13}^2}{c_{11}} \frac{1}{4g(1-g)} \Gamma_P; \\
C_{44}^{OA-str} &\approx c_{44}; & C_{55}^{OA-str} &\approx c_{44}(1-\Delta_T) + c_{44}\Gamma_S; & C_{66}^{OA-str} &\approx c_{66}(1-\Delta_H)
\end{aligned} \tag{5}$$

2.2 Approximate equation construction and response analysis

This section uses asymptotic ray theory to linearize the PP wave reflection coefficient and express its amplitude change with the incident angle and azimuth as a function of the scattering function $S(\theta, \varphi)$. According to the Shaw approximation, the PP wave reflection coefficient $R_{PP}(\theta, \varphi)$ can be expressed by the scattering function $S(\theta, \varphi)$ as [18]:

$$R_{PP}(\theta, \varphi) = \frac{1}{4\rho \cos^2 \theta} S(\theta, \varphi) \quad (6)$$

where θ and φ represent the incident angle and azimuth, respectively, and ρ represents the density of the medium. The scattering function $S(\theta, \varphi)$ can be expressed as:

$$S(\theta, \varphi) = \Delta\rho \cos 2\theta + \sum_{i=1}^6 \sum_{j=1}^6 \Delta C_{ij}^{str} \eta_{ij} \quad (7)$$

Δ represents the disturbance of the elastic properties of stress-free or stress-loaded rock, $\Delta\rho$ represents the disturbance term of density, and η_{ij} is related to the slowness and polarization vector of the incident P wave and the reflected P wave. It is the product of the slowness and the polarization vector and can be expressed as $\eta_{ij} = \eta_{ijkl} = \dot{p}_i \dot{s}_j p_k s_l$. Where p_k and \dot{p}_i represent the polarization vectors of the incident wave and the reflected wave, and s_l and \dot{s}_j represent the slowness vectors of the incident wave and the reflected wave, respectively. ΔC_{ij}^{str} represents the perturbation stiffness coefficient matrix of the OA medium under the initial stress. The specific components can be expressed as:

$$\begin{aligned} \Delta C_{11}^{str} &= \Delta C_{11} - C_{11} \Delta\delta_N + C_{11} \frac{1}{4g(1-g)} \Delta\Gamma_P; & \Delta C_{12}^{str} &= \Delta C_{12} - C_{12} \Delta\delta_N + C_{12} \frac{1}{4g(1-g)} \Delta\Gamma_P; \\ \Delta C_{13}^{str} &= \Delta C_{13} - C_{13} \Delta\delta_N + C_{13} \frac{1}{4g(1-g)} \Delta\Gamma_P; & \Delta C_{22}^{str} &= \Delta C_{11} \frac{C_{12}^2}{C_{11}} \Delta\delta_N + \frac{C_{12}^2}{C_{11}} \frac{1}{4g(1-g)} \Delta\Gamma_P; \\ \Delta C_{23}^{str} &= \Delta C_{13} - \frac{C_{12} C_{13}}{C_{11}} \Delta\delta_N + \frac{C_{12} C_{13}}{C_{11}} \frac{1}{4g(1-g)} \Delta\Gamma_P; & \Delta C_{33}^{str} &= \Delta C_{33} - \frac{C_B^2}{C_{11}} \Delta\delta_N + \frac{C_{13}^2}{C_{11}} \frac{1}{4g(1-g)} \Delta\Gamma_P; \\ \Delta C_{55}^{str} &= \Delta C_{44} - C_{44} \Delta\delta_V + C_{44} \Delta\Gamma_S; & \Delta C_{66}^{str} &= \Delta C_{66} - C_{66} \Delta\delta_H; & \Delta C_{44}^{str} &= \Delta C_{44} \end{aligned} \quad (9)$$

In order to avoid confusion in understanding, the perturbation terms of Δ_N , Δ_T and Δ_H are expressed as $\Delta\delta_N$, $\Delta\delta_T$ and $\Delta\delta_H$ in the calculation process. The stiffness coefficient without the str superscript represents the stiffness coefficient of the background medium (VTI medium) and the perturbation term of the stiffness coefficient. In order to make the equation finally not contain the stiffness coefficient matrix of the background medium and its perturbation, the velocity, density and anisotropy parameters of the VTI medium can be used to express its stiffness coefficient and stiffness coefficient perturbation as:

$$\begin{aligned} C_{33} &= V_P^2 \rho; & \Delta C_{33} &= 2\Delta V_P V_P \rho + V_P^2 \Delta\rho; & C_{44} &= V_S^2 \rho; & \Delta C_{44} &= 2\Delta V_S V_S \rho + V_S^2 \Delta\rho; \\ C_{11} &= V_P^2 \rho (2\varepsilon + 1); & \Delta C_{11} &= (2\Delta V_P V_P \rho + V_P^2 \Delta\rho) (2\varepsilon + 1) + 2\Delta\varepsilon V_P^2 \rho; \\ C_{66} &= V_S^2 \rho (2\gamma + 1); & \Delta C_{66} &= (2\Delta V_S V_S \rho + V_S^2 \Delta\rho) (2\gamma + 1) + 2\Delta\gamma V_S^2 \rho; \\ C_{13} &= V_P^2 \rho \delta + (V_P^2 \rho - 2V_S^2 \rho); & \Delta C_{13} &= (2\Delta V_P V_P \rho + V_P^2 \Delta\rho) (\delta + 1) + 2\Delta\delta V_P^2 \rho - 2(2\Delta V_S V_S \rho + V_S^2 \Delta\rho) \\ C_{12} &= C_{11} - 2C_{66} & \Delta C_{12} &= \Delta C_{11} - 2\Delta C_{66} \end{aligned} \quad (10)$$

where ε , δ and γ are the anisotropy parameters in the VTI medium without initial stress. Substituting the obtained parameters into (6) and (7), the PP wave reflection coefficient can be obtained according to equation (6). And using equation (10) and a series of simplification rules such as $g = \frac{V_S^2}{V_P^2}$, $\frac{\Delta V_S}{V_P} = 2gR_{V_S}$ combining (8) and (10) and substituting them into (6), the PP wave approximate reflection coefficient equation considering the decoupling of fracture-induced

anisotropy and stress-induced anisotropy of OA medium under the action of initial stress can be obtained:

$$R_{PP}(\theta, \varphi) = A_M(\theta) R_M + A_\mu(\theta) R_\mu + A_{rho}(\theta) R_{rho} + A_{\delta_b}(\theta) R_{\delta_b} + A_{\varepsilon_b}(\theta) R_{\varepsilon_b} \dots \\ + A_N(\theta, \varphi) R_{\delta_N} + A_T(\theta, \varphi) R_{\delta_T} + A_H(\theta, \varphi) R_{\delta_H} + A_P(\theta, \varphi) R_{\Gamma_P} + A_S(\theta, \varphi) R_{\Gamma_S} \quad (11)$$

At this time, the reflection coefficient equation has a total of 10 parameters to be inverted. Too many inversion parameters are not conducive to the subsequent inversion, and the parameters need to be simplified. Assuming that the fracture is a rotationally invariant fracture $\delta_T = \delta_H$ can be obtained. At the same time, assuming that the reservoir is a gas-bearing reservoir [19], the normal and tangential fracture parameters have the following relationship: $\delta_T = \frac{4g(1-g)}{3-2g} \delta_N$. Based on the above assumptions, equation (11) can be rewritten as:

$$R_{PP}(\theta, \varphi) = A_M(\theta) R_M + A_\mu(\theta) R_\mu + A_{rho}(\theta) R_{rho} + A_{\delta_b}(\theta) R_{\delta_b} + A_{\varepsilon_b}(\theta) R_{\varepsilon_b} \dots \\ + A_N(\theta, \varphi) R_{\delta_N} + A_P(\theta, \varphi) R_{\Gamma_P} + A_S(\theta, \varphi) R_{\Gamma_S} \quad (12)$$

Where:

$$A_P(\theta, \varphi) = \frac{1}{8(-1+g)g \cos^2 \theta} \left(1 + 4g^2 \cos^4 \theta + 4g \cos^2 \theta \left(\frac{-1+g \cos^4 \varphi \sin^2 \theta \tan^2 \theta + \cos^2 \varphi}{(-\tan^2 \theta + \sin^2 \theta (2g + \sin^2 \varphi \tan^2 \theta))} \right) \right); \\ A_N(\theta, \varphi) = \frac{1}{4(-3+2g) \cos^2 \theta} \left(\frac{3-2g+4(3-2g)g^2 \cos^4 \theta - 4g \cos^2 \theta}{\left((3-2g)(-1+g \cos^4 \varphi \sin^2 \theta \tan^2 \theta) + \cos^2 \varphi \right)} \right); \quad (13) \\ A_\mu(\theta) = -2g \sin^2 \theta; \quad A_M(\theta) = \frac{1}{4 \cos^2 \theta}; \quad A_{rho}(\theta) = \frac{\cos^2 \theta - \sin^2 \theta}{4 \cos^2 \theta}; \\ A_S(\theta, \varphi) = 2g \cos^2 \varphi \tan^2 \theta; \quad A_{\delta_b}(\theta) = \frac{1}{2} \sin^2 \theta; \quad A_{\varepsilon_b}(\theta) = \frac{\tan^2 \theta \sin^2 \theta}{2}$$

Where $R_M = \frac{\Delta M}{M}$, $R_\mu = \frac{\Delta \mu}{\mu}$, $R_\rho = \frac{\Delta \rho}{\rho}$, $R_{\delta_b} = \Delta \delta_b$, $R_{\varepsilon_b} = \Delta \varepsilon_b$, $R_{\delta_N} = \Delta \delta_N$, $R_{\Gamma_P} = \Delta \Gamma_P$, $R_{\Gamma_S} = \Delta \Gamma_S$. \bar{M} , $\bar{\mu}$, $\bar{\rho}$ represent the longitudinal wave modulus, shear modulus and density respectively. The longitudinal wave modulus can be expressed as $M = \lambda + 2\mu = V_p^2 \rho$, and the shear modulus can be expressed as $\mu = V_s^2 \rho$. ΔM , $\Delta \mu$, and $\Delta \rho$ represent the perturbations of the longitudinal and shear wave velocities and density respectively. $\Delta \varepsilon_b$ and $\Delta \delta_b$ represent the perturbations of the anisotropic parameters of the background medium respectively. $\Delta \delta_N$ represents the perturbation value of the fracture normal phase weakness. $\Delta \Gamma_P$ and $\Delta \Gamma_S$ represent the perturbations of the P-wave and S-wave stress terms respectively.

The azimuth amplitude difference method is used in the inversion process. Different azimuth seismic amplitudes are used to make differences to eliminate the influence of the background medium and retain the anisotropic information caused by cracks and stress. At this time, only three parameters are related to the azimuth angle to be inverted. After obtaining the three azimuth angle-related parameters, the inversion of five isotropic terms is performed. This inversion strategy can reduce the time of the inversion algorithm and increase the credibility of the inversion results.

3. Model testing and work area application

(1) Model Testing

In order to verify the feasibility of using the amplitude difference of azimuth seismic data to invert fracture weakness and stress action terms, the model inversion was performed using the single-channel data corresponding to a well. In the simulation test, the wavelet used the Ricker

wavelet with a main frequency of 30 Hz, an incident angle range of $0^\circ \sim 45^\circ$, and the azimuth seismic data selected were partial stacking azimuth seismic data with average angles of $\varphi_1=15^\circ$, $\varphi_2=75^\circ$, $\varphi_3=105^\circ$, and $\varphi_4=165^\circ$. In order to verify the stability, Gaussian random noise was added to the azimuth seismic data, with signal-to-noise ratios of 2: 1 and 5: 1, respectively. The azimuth amplitude difference data of $\varphi_2 - \varphi_1$, $\varphi_3 - \varphi_2$, and $\varphi_4 - \varphi_3$ were used to invert the normal fracture weakness and the stress terms of P and S waves. After obtaining the inversion results of anisotropic information, the longitudinal wave modulus, shear modulus, density, and background medium anisotropic parameters were predicted based on the inversion results of fracture weakness and stress terms. In the figure below, the red dotted line represents the inversion result, the blue line represents the actual data, and the black line represents the input low-frequency model. According to Fig. 1-a, it can be seen that in the absence of noise interference, the inversion effect is highly consistent with the actual model, which can verify the rationality of the method; according to Fig. 1-b and Fig. 1-c, it can be analyzed that under the interference of noise with different signal-to-noise ratios, the inversion results are still highly consistent with the actual data, which can prove the feasibility of the method.

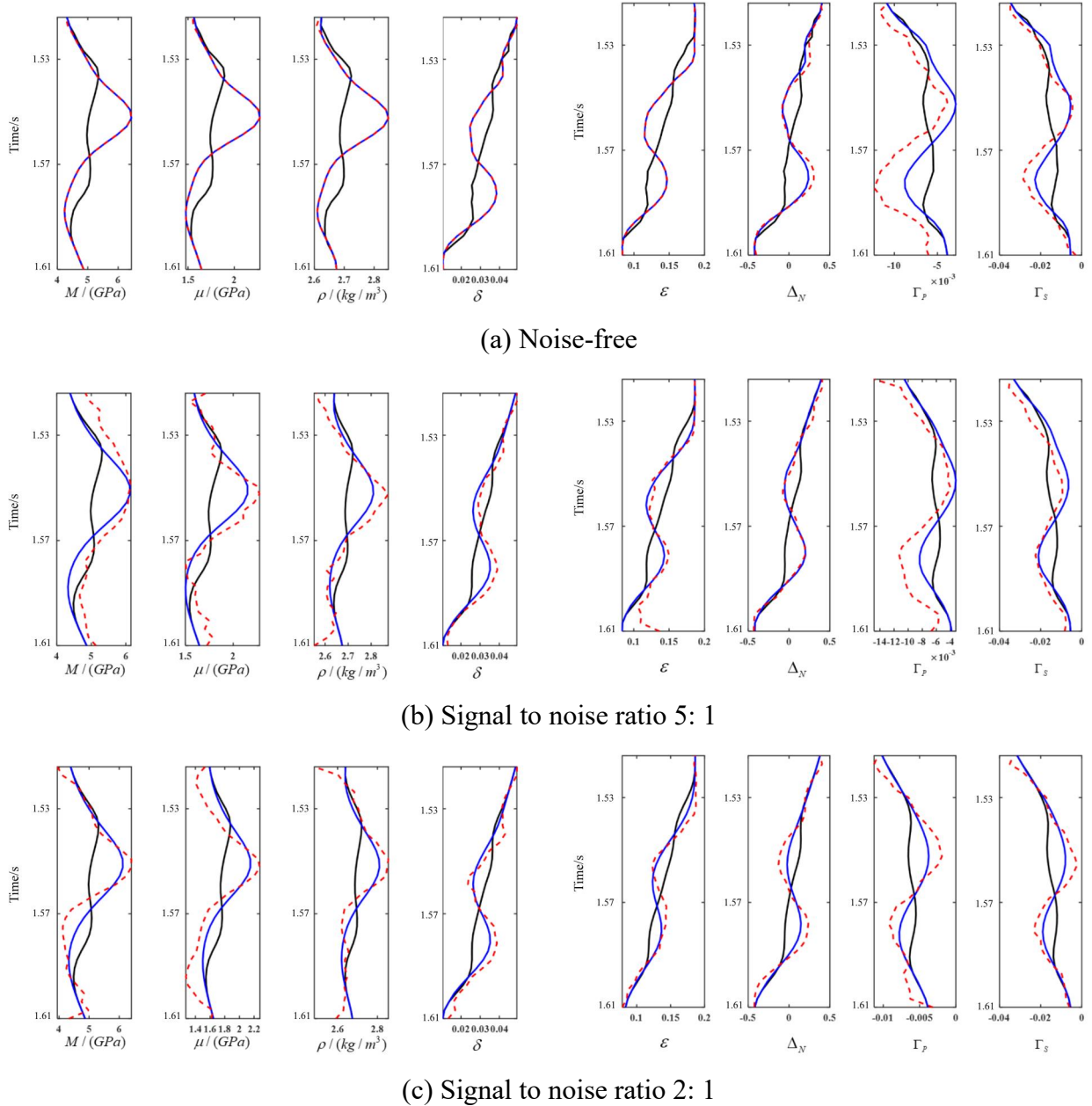


Fig. 1 Inversion results with different signal-to-noise ratios

(2) Actual work area application

The actual application area is a shale reservoir with vertical fractures and OA medium characteristics, and the main reservoir is a gas-bearing reservoir. In line with the assumptions made in the theoretical derivation process for practical situations, the application verification and analysis of the azimuth amplitude difference inversion method can be carried out. The seismic data is partially stacked using two azimuth angles: $\varphi_1 = 45^\circ$ (stack range $30^\circ \sim 60^\circ$) and $\varphi_2 = 135^\circ$ (stack range $120^\circ \sim 150^\circ$), where three incident angles of 10° , 20° , and 30° are selected for each azimuth. $\varphi_2 - \varphi_1$, $\varphi_3 - \varphi_2$, and $\varphi_4 - \varphi_3$ are selected as azimuth amplitude difference seismic data, and the background medium's Thomsen anisotropy parameters are obtained using the layer constraint and well interpolation. The stress action term and normal fracture weakness are calculated using the Thomsen anisotropy parameters as the low-frequency model. Fig. 2 shows the inversion effect of elastic data independent of azimuth data, and Fig. 3 shows the azimuth-related fracture weakness and stress terms. The black curve is the curve of the corresponding parameters on the well. The inversion result corresponds well to the well curve, proving the method's feasibility.

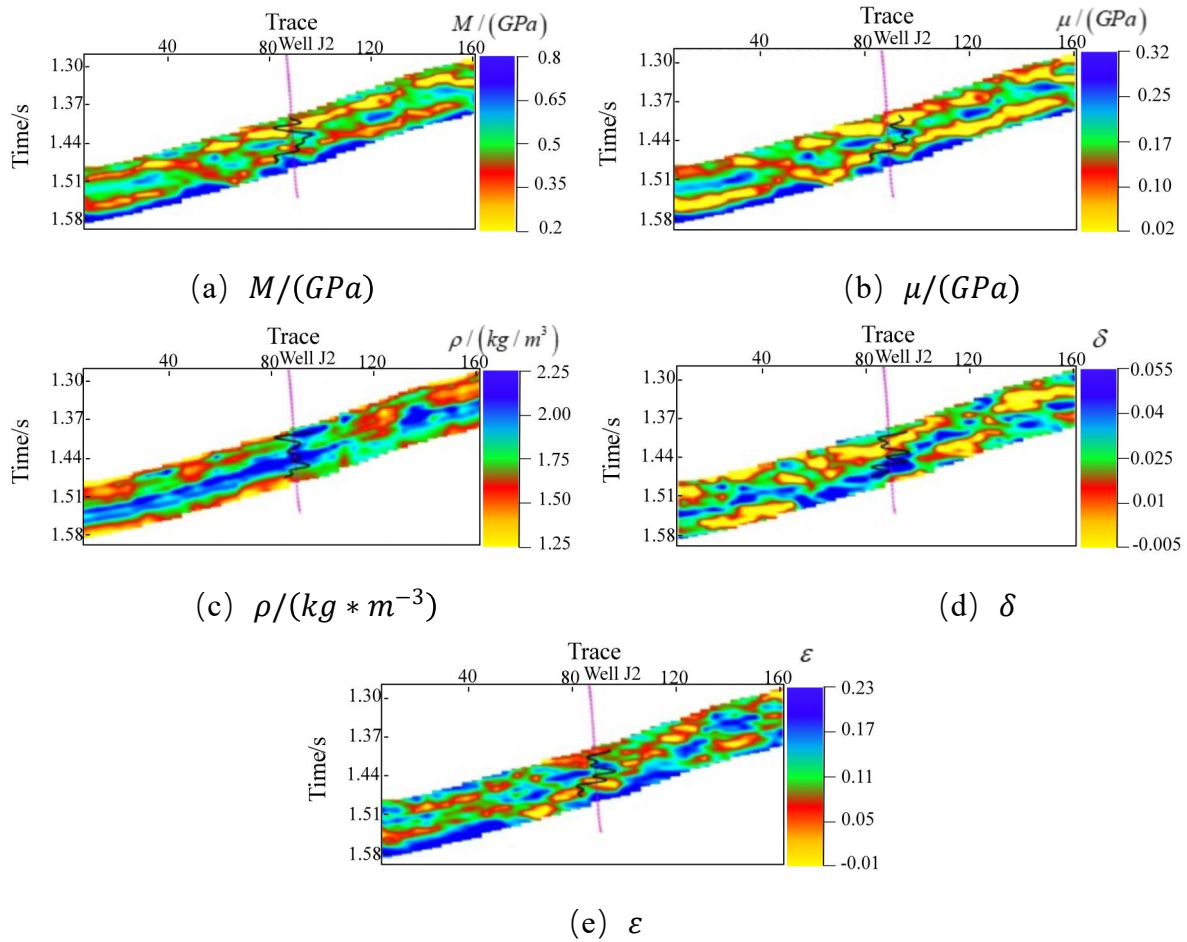
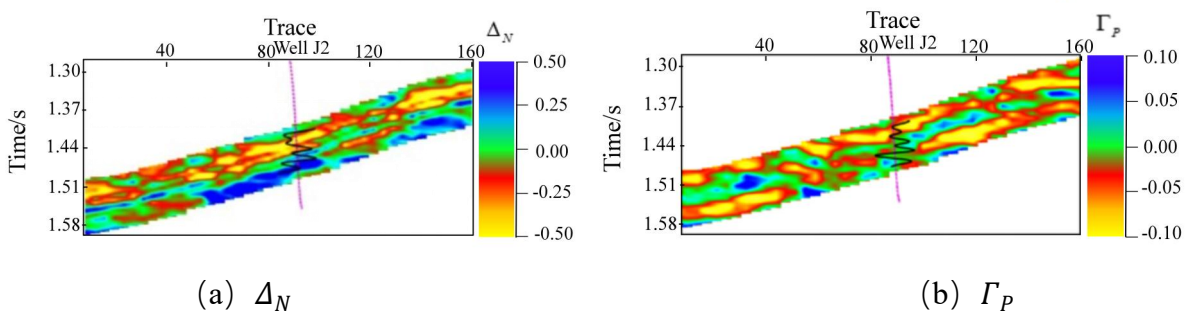


Fig. 2 Isotropic coefficient inversion results section at different azimuth angles



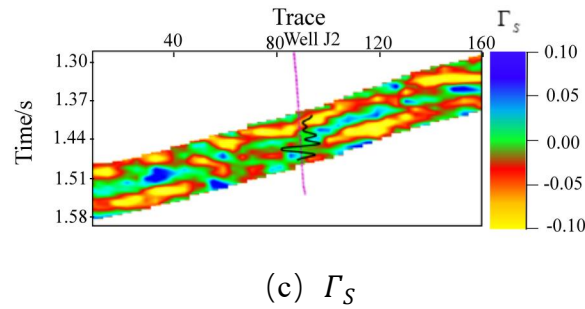


Fig. 3 Section of the anisotropy coefficient inversion results at different azimuth angles

4. Summary

In order to explore the influence of cracks and stress in the medium and improve the efficiency of seismic inversion, an approximate equation was constructed based on the Born first-order approximation, and the approximate equation inversion method of OA medium under initial stress was studied. The approximate equation inversion based on the Bayesian framework was attempted. The feasibility of this method in predicting crack and stress parameters was verified in model testing and actual data application. However, due to the large number of inversion parameters and high requirements for seismic data, improving the inversion accuracy and reducing the requirements for seismic data are issues that need to be solved in the future.

Acknowledgements

The authors acknowledge the sponsorship of National Natural Science Foundation of China (42174139, 41974119, 42030103), The Marine Science and Technology Fund of Shandong Province Marine Science and Technology Pilot National Laboratory (Qingdao) (2021QNLM020001-6), and Science Foundation from Innovation and Technology Support Program for Young Scientists in Colleges of Shandong Province and Ministry of Science and Technology of China (2019RA2136).

References

- [1] CHEN F, ZONG Z, JIANG M. Seismic reflectivity and transmissivity parametrization with the effect of normal in situ stress [J]. *Geophysical Journal International*, 2021, 226(3): 1599-614.
- [2] MULARGIA F. The evaluation of Murnaghan constants as a function of pressure [J]. *Lettere al Nuovo Cimento* (1971-1985), 1979, 26(15): 471-6.
- [3] TRAYLOR T K, BURNLEY P C, WHITAKER M. Initial Acoustoelastic Measurements in Olivine: Investigating the Effect of Stress on P - and S - Wave Velocities [J]. *Journal of Geophysical Research: Solid Earth*, 2021, 126(11): e2021JB022494.
- [4] THURSTON R, BRUGGER K. Third-order elastic constants and the velocity of small amplitude elastic waves in homogeneously stressed media [J]. *Physical Review*, 1964, 133(6A): A1604.
- [5] TOUPIN R, BERNSTEIN B. Sound waves in deformed perfectly elastic materials. Acoustoelastic effect [J]. *The Journal of the Acoustical Society of America*, 1961, 33(2): 216-25.
- [6] CRECRAFT D. The measurement of applied and residual stresses in metals using ultrasonic waves [J]. *Journal of Sound and Vibration*, 1967, 5(1): 173-92.
- [7] PAO Y-H. Acoustoelasticity and ultrasonic measurements of residual stresses [J]. *Physical acoustics XVII*, 1984: 61-143.
- [8] THURSTON R. Waves in solids [J]. In: *Mechanics of solids IV (Festkoerpermechanik IV)* Berlin, 1974, 4: 109-308.
- [9] WINKLER K W, LIU X. Measurements of third - order elastic constants in rocks [J]. *The Journal of the Acoustical Society of America*, 1996, 100(3): 1392-8.

- [10] WINKLER K W. Azimuthal velocity variations caused by borehole stress concentrations [J]. *Journal of Geophysical Research: Solid Earth*, 1996, 101(B4): 8615-21.
- [11] SINHA B K, KOSTEK S. Stress-induced azimuthal anisotropy in borehole flexural waves [J]. *Geophysics*, 1996, 61(6): 1899-907.
- [12] GRAY D, TODOROVIC-MARINIC D. Fracture detection using 3D azimuthal AVO [J]. *CSEG Recorder*, 2004, 29(10): 5-8.
- [13] ZONG Z, YIN X, WU G. AVAZ inversion and stress evaluation in heterogeneous medium; proceedings of the SEG International Exposition and Annual Meeting, Houston, F, 2013 [C]. SEG.
- [14] MAHMOUDIAN F, MARGRAVE G F. AVAZ Inversion for Fracture Orientation and Intensity-A Physical Modeling Study; proceedings of the 75th EAGE Conference & Exhibition incorporating SPE EUROPEC 2013, London, F, 2013 [C]. European Association of Geoscientists & Engineers.
- [15] 张广智, 杜炳毅, 李海山, et al. 页岩气储层纵横波叠前联合反演方法 [J]. *地球物理学报*, 2014, 57(12): 4141-9.
- [16] 陈怀震, 印兴耀, 高建虎, et al. 基于等效各向异性和流体替换的地下裂缝地震预测方法 [J]. *中国科学: 地球科学*, 2015, (5): 589-600.
- [17] SARKAR D, BAKULIN A, KRANZ R L. Anisotropic inversion of seismic data for stressed media: Theory and a physical modeling study on Berea Sandstone [J]. *Geophysics*, 2003, 68(2): 690-704.
- [18] PAN X, ZHAO Z. A Decoupled Fracture- and Stress-Induced PP-wave Reflection Coefficient Approximation for Azimuthal Seismic Inversion in Stressed Horizontal Transversely Isotropic Media [J]. *Surveys in Geophysics*, 2023, 45(1): 151-82.
- [19] BAKULIN A, GRECHKA V, TSVANKIN I. Estimation of fracture parameters from reflection seismic data—Part III: Fractured models with monoclinic symmetry [J]. *Geophysics*, 2000, 65(6): 1818-30.